Maximal Dynamic Range Electrotactile Stimulation Waveforms

Kurt A. Kaczmarek, *Member, IEEE*, John G. Webster, *Fellow, IEEE*, Robert G. Radwin, *Member, IEEE*

Abstract—**A new method to measure the dynamic range of electrotactile (electrocutaneous) stimulation uses both steepest ascent (gradient) and one-variable-at-a-time methods to determine the waveform variables that maximize the subjective magnitude (intensity) of the electrotactile percept at the maximal current without discomfort for balanced-biphasic pulse bursts presented at a 15-Hz rate. The magnitude at the maximal current without discomfort is maximized by the following waveform (range tested in parentheses): number of pulses/burst = 6 (1–20), pulse repetition rate within a burst = 350 Hz (200–1500), and phase width = 150 μs (40–350). The interphase interval (separation between positive and negative phases in a biphasic pulse) does not affect dynamic range from 0–500 μs.**

The number of pulses/burst has a large effect on the perceived dynamic range when this is measured using a subjective-magnitude-based algorithm, whereas it has little effect on the traditional dynamic range measure, i.e., (maximal current without discomfort)/(sensation threshold current). The perceived stimulus magnitude at the maximal current without discomfort is approximately twice as strong with 6 pulses/burst as it is with 1 pulse/burst (a frequently-used waveform).

Introduction

Background

Electrotactile stimulation evokes tactile (touch) sensations within the skin at the location of the electrode by passing a local electric current through the skin. Sensory substitution is the use of one human sense (in this case, touch) to receive environmental information normally received by another sense (often vision or hearing). For the sense of touch, sensory substitution is the use of one area of skin to receive tactile information normally received at another location. Several articles review technology and devices for electrotactile stimulation [1]–[3], visual substitution [4], [5], auditory substitution [6]–[8], and other applications [2], [3], [9]–[12].

Dynamic Range

A limitation of present electrotactile displays is that they lack a large comfortable sensation magnitude; this can limit their effectiveness in certain applications. Our normal senses of vision, hearing, and touch can mediate stimuli that we perceive as strong or intense without being painful. Electrotactile stimulation, on the other hand, can develop an uncomfortable stinging quality even at moderate stimulation levels if improper stimulation waveforms or electrodes are used.

The traditional measure of electrotactile intensity dynamic range is the ratio of the stimulation *currents* required to produce sensation threshold S and pain threshold P (mA). The ratio P/S typically ranges from 2–4 for unexperienced observers (O's) and 6–8 for experienced O's [13]. (This range is a limitation for magnitude-modulated stimulation codes but not necessarily for frequency or spatially-modulated codes.) However, P, S, and by extension P/S are *electrical* measures; they give limited information about the *percept* produced by stimulation. Choosing a stimulation waveform that maximizes P/S does not guarantee a usefully-strong or comfortable sensation.

We propose that a better measure of the dynamic range of a tactile display is the range of *perceived* stimulation magnitudes that are both perceptible and comfortable, from the magnitude at the sensation threshold current $\psi(S)$ to the (maximal) magnitude at the maximal current without discomfort $\Gamma \equiv \psi(M)$. We chose M instead of the pain threshold P to avoid any stimulations described as uncomfortable or painful because eventual users of a practical sensory substitution system would not likely accept such sensations. For five O's (not the same set as for the experiments to be described), P/M varied from 1.1 to 1.6, with a mean value of 1.3.

The actual stimulus percept is a psychophysical function of all the waveform and electrode variables, including the current I. One aspect of the stimulus percept is its subjective intensity or magnitude, typically designated by ψ. It can be described by Stevens' power law [14], [15]:

$$\psi = (I - S)^n$$

where S is the sensation threshold current (which is sometimes set arbitrarily to zero—inappropriate in our view for electrotactile stimulation in which S is not small compared with I), and I is the stimulus current. Note that by this definition, the magnitude at sensation threshold $\psi(S) = 0$. The exponent n has been reported to range from 0.9 to 3.5 [16], [17]. The range of n values is due to several factors. 1) Stimulation of nerve bundles (e.g., the median

Manuscript received June 6, 1991; revised January 30, 1992. This work was supported by the National Institutes of Health Grant NS26328.

K. A. Kaczmarek and J. G. Webster are with the Department of Electrical and Computer Engineering, University of Wisconsin, Madison, WI 53706.

R. G. Radwin is with the Department of Industrial Engineering, University of Wisconsin, Madison, WI 53706.

IEEE Log Number 9200698.

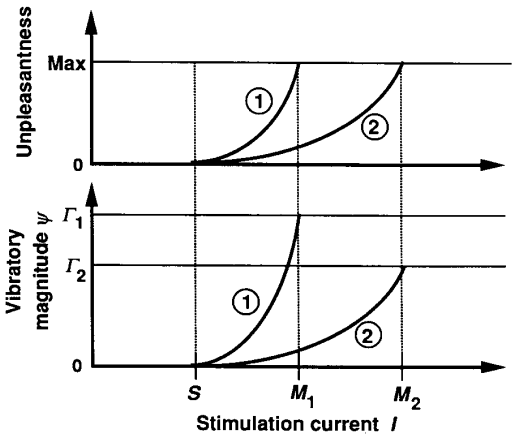

Fig. 1. Two qualities of electrotactile stimulation are vibratory magnitude ψ and unpleasantness. Condition 1 has a greater dynamic range than condition 2 because $\Gamma_1 > \Gamma_2$, even if $M_1/S < M_2/S$. The maximal current without discomfort M for each case is limited by the maximal acceptable unpleasantness in the electrotactile percept. S is the sensation threshold current.

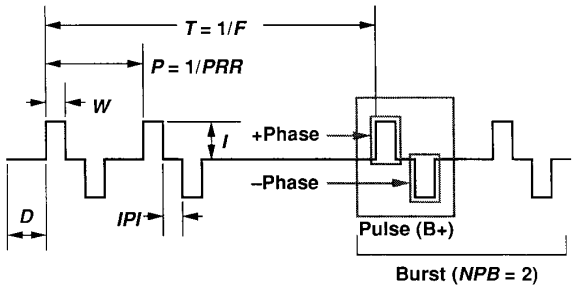

Fig. 2. Electrotactile waveform variables: D, delay; W, width; IPI, interphase interval; I, current; T, time between bursts; F, frequency of burst repetition; P, period of pulse repetition; PRR, pulse repetition rate; NPB, number of pulses per burst.

nerve at the wrist) produces a much different nonlocalized percept than stimulation of localized areas of skin (our method), which can produce a vibratory percept similar to normal touch. 2) Some studies assume *a priori* that electrotactile stimulation is uncomfortable by using such terms as "shock," and ask the observer to rate discomfort magnitude rather than tactile magnitude. Studies measuring tactile magnitude and discomfort magnitude cannot be directly compared because the dependent variables are different. 3) The calculated value of n varies depending on the overall range of stimulation intensities and other experimental biases [16]. 4) A power function may not provide the best description of the relationship between ψ and I [18]. The present studies do not intrinsically depend on any particular function.

Furthermore, we distinguish between the (vibratory) tactile magnitude ψ and another aspect of the stimulus percept: its degree of "unpleasantness" or "sting." Fig. 1 qualitatively shows that at one set of stimulation waveform variables (condition 2) the ratio $\Re_2 = M_2/S$ is high but the magnitude Γ_2 is low. Condition 1 represents a potentially better operating range; while $\Re_1$ is smaller, Γ_1 is higher than for condition 2, i.e., the range of perceived stimulation intensities $\Gamma - \psi(S) = \Gamma$ is larger. Therefore, we believe that Γ is a better measure of dynamic range than $\Re$. If Γ is maximized, the entire range of stimulation intensities is maximally comfortable. The purpose of this study is to determine the set of waveform variables that maximize Γ. Note that while ψ is dependent on the stimulus current I, Γ is not. By definition, Γ is measured at the predetermined maximal current that is not uncomfortable, e.g., $\Gamma \equiv \psi(M)$.

Materials and Methods

Nomenclature

Waveforms: For balanced-biphasic current pulses, seven stimulation waveform variables influence the electrotactile sensation (Fig. 2). Note that the two *phases* of a *balanced-biphasic* waveform pulse are often called *pulses* (with the result that interphase interval IPI is called "interpulse interval"). Introducing the term "phase" avoids the above ambiguity [19].

Numerical Notation: Many experimental measurements are repeated and averaged to improve precision and assess repeatability. A quantity $x_{rj}(\boldsymbol{w})$ is measured with the stimulation waveform $\boldsymbol{w}$. (Boldface notation denotes between the general waveform vector quantity $\boldsymbol{w}$, which is the set of all applicable waveform variables (except current) in Fig. 2. In these experiments, only NPB, PRR, W, and IPI vary; F is fixed at 15 Hz and D is zero.) In several experiments, most of the waveform variables are held fixed and only one is varied, in which case $\boldsymbol{w}$ becomes the scalar k.

The measurements are taken in sets or replications r where $r = 1, 2 \cdots R$. Within each replication, the trial number j indicates the actual (random) order of measurements where $j = 1 \cdots J$. Therefore, an individual measurement x can be uniquely specified with either x_{rj}—the jth trial in the rth replication, or with $x_r(\boldsymbol{w})$—the waveform $\boldsymbol{w}$ in the rth replication. When data are averaged, an overbar specifies the variable that is an average and a dot replaces the variable that is averaged over. For example

$$\bar{x}_{\cdot}(\boldsymbol{w}) = \frac{1}{R}\sum_{r=1}^{R} x_r(\boldsymbol{w})$$

specifies the mean of all R replications of x with waveform $\boldsymbol{w}$.

Dependent and Independent Variables: The dependent variables in this set of experiments are 1) the sensation threshold current S (mA), 2) the maximal current without discomfort M (mA), 3) the estimated magnitude (intensity, strength) ψ, and 4) the estimated magnitude at the maximal current without discomfort $\Gamma(\boldsymbol{w}) \equiv \psi[\boldsymbol{w}, M(\boldsymbol{w})]$. We emphasize that Γ is the magnitude at the *predetermined* current M, and that it is a function of $\boldsymbol{w}$. The numeric magnitude estimates ψ were entered by O on the keyboard. Because some experiments measured all of S, M, and Γ, we respectively use U, V, and R to denote the number of replications u, v, and r for each.

Where data from more than one O combine in one

expression, a second comma-separated subscript o denotes the observer; e.g., $S_{rj,o}(\boldsymbol{w})$ is the sensation threshold for the rth replication on the oth observer for waveform $\boldsymbol{w}$; j is the trial corresponding to waveform $\boldsymbol{w}$. Finally, nonnumeric subscripts denote a specific stimulation condition (independent variable) rather than a replication or trial number. For example, $\mathrm{NPB}_{\mathrm{REF}}$ is the value of NPB for a reference stimulus REF. The small caps notation denotes a specific stimulation condition. Measured quantities (dependent variables) do not use this notation.

Instrumentation

Waveform generator: A computer-controlled electrotactile stimulation system [19] automatically delivered the desired stimulation, prompted the observer for responses, and then logged O's responses. For determination of the sensation threshold current S and the maximal current without discomfort M, a knob manipulated by O's left hand controlled the stimulation current according to

$$I = (x - rnd)A$$

where I is the stimulation current in mA (clamped so that $I \geq 0$), $x \geq 0$), x is the knob rotation (full range from 0 to 1), and A is a scaling factor that causes O to use the middle 60% of the knob range. Subtracting the random knob offset *rnd* (range 0–0.2) prevents O from using the knob rotation as a cue for determining S and M.

Electrode: At the beginning of each experimental session, O waited 5 min for the electrode–skin interface to stabilize after placing the electrode belt on moistened skin. The current-controlled pulses were delivered to O's tap-water-premoistened abdomen by the twelfth electrode from the left (cable side) in the elasticized-belt linear electrode array from a Tacticon™ auditory prosthesis for the deaf [12], [20], [21]. The 5.5-mm-diameter gold-plated electrodes are surrounded by the conductive rubber base material of the belt, which serves as a ground plane. The electrode site was approximately 2 cm above and 7 cm right of the navel. For O's with dense hair or bony protuberances at this location that prevented proper electrode contact (as evidenced by sharp, prickly electrotactile sensations), we relocated the electrode laterally to a smoother location. Occasionally the chosen site would yield prickly sensations or muscle contractions for no apparent reason; this was readily corrected by moving the electrode a few millimeters in any direction and re-wetting the skin. On particularly dry winter days with indoor relative humidity below 30%, a steam humidifier under the experiment station desk maintained sufficient abdominal skin hydration by keeping the humidity between 20 and 40% near O. Insufficient skin hydration causes prickly sensations, probably because of nonuniform current density at the electrode–skin interface [1].

Observers

Ten O's (three female and seven male, ages 19–30 with varied ethnic backgrounds) initially participated in this study. One female and two males were dismissed after the first experimental session due to unrepeatable results (Appendix A). O's received $5.00/h payment, and were recruited by personal contact and posters in University buildings. Observers 1, 3, and 6 respectively had 7, 15, and 50 h prior experience with electrotactile stimulation; the others had none.

Optimization Scheme

The objective of the following set of experiments, identified by boldface names, was to refine an initial guess *Baseline 1* of the optimal waveform $\boldsymbol{w}$ that maximizes the dynamic range Γ. Several types of experiments gathered information for screening O's and systematically maximizing Γ. **Scale 1, Scale 2,** and **Scale 3,** using slightly different procedures, determined the relationship between the stimulation current I and the subjective magnitude ψ. **MagNPBscreen** measured the maximal magnitude Γ(NPB) at the maximal current without discomfort M(NPB). Because preliminary unpublished data established that Γ depends on NPB, **MagNPBscreen** and **Scale 1** screened observers by testing their ability to repeatably determine M, ψ, and Γ (Appendix A).

Fig. 3 illustrates in two dimensions the procedure used to maximize Γ in the four-dimensional space $\boldsymbol{w} \equiv$ (NPB, PRR, W, IPI). With seven suitable O's, **Gradient** determined the direction of steepest ascent $\nabla\Gamma(\boldsymbol{w})$ at the first guess of $\boldsymbol{w}$ = *Baseline 1*. (Preliminary unpublished experiments similar to those to be described provided the value of *Baseline 1*.) Then **Search** varied $\boldsymbol{w}$ in the direction of $\nabla\Gamma(\boldsymbol{w})$, starting at *Baseline 1*, to estimate the value of $\boldsymbol{w}$ that maximized $\Gamma(\boldsymbol{w})$. This value of $\boldsymbol{w}$ is *Baseline 2*. **Gradient** also supplied information on how the effects of NPB, PRR, W, and IPI interacted, i.e., how the value of one of these variables influenced the effect of the others on Γ.

Finally, **MagNPB**, **MagPRR**, **MagW** and **MagIPI** varied each of these four variables separately around *Baseline 2* to investigate the detailed response of $\Gamma(\boldsymbol{w})$. A final adjustment in $\boldsymbol{w}$ based on these four experiments provided the best approximation of the optimal $\boldsymbol{w}$.

Order of Experiments

Each of the seven O's completed four experimental sessions on different days at varying times but in the following order (except O1 did not complete session 4):

First session (2 h):	**Scale 1** and **MagNPBscreen**
Second session (2.5 h):	**Scale 2, Gradient,** and **Search**
Third session (2 h):	**Scale 3** and two of the following: **MagNPB, MagPRR, MagW,** and **MagIPI**
Fourth session (2 h):	**Scale 3** and the remaining two of the following: **MagNPB, MagPRR, MagW,** and **MagIPI**

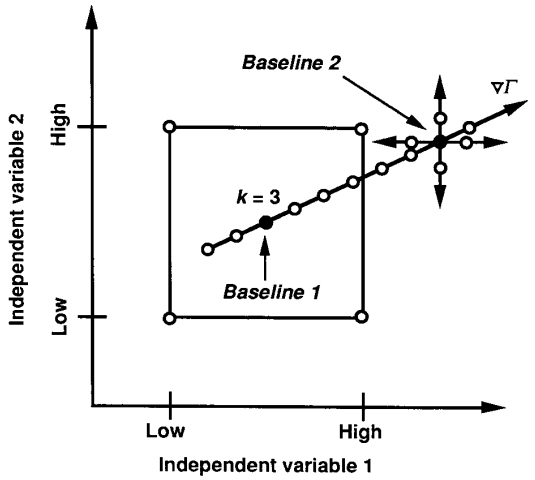

Fig. 3. The optimization procedure finds the waveform w which maximizes the dynamic range $\Gamma(w)$. We show two of the four dimensions in the space of independent variables (NPB, PRR, W, IPI). The procedure starts by finding the gradient $\nabla\Gamma(w)$ at the first approximation of the optimal w = *Baseline 1*. $\Gamma(k)$ is measured along the gradient path (a 1-dimensional subspace of w). The value of k which maximizes $\Gamma(w)$ defines w = *Baseline 2*. The four independent variables are then varied one-at-a-time around *Baseline 2* to explore this region and determine the final optimum. With the fixed waveform value of F = 15 Hz, *Baseline 1* = (6 pulses/burst, 400 Hz, 100 μs, 100 μs). With the same units, *Baseline 2* = (7, 400, 120, 100) and the final optimal waveform is (6, 350, 150, IPI) where IPI has no effect on Γ.

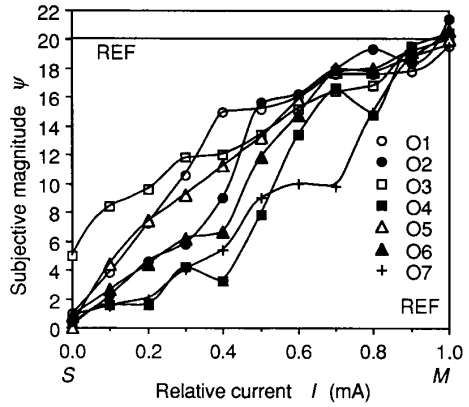

Fig. 4. **Scale 1:** Subjective magnitude ψ increases approximately linearly with stimulation current I for 7 observers. S is the sensation threshold current and M is the maximal current without discomfort. A reference current I_{REF} (magnitude 20) is presented to the observer before each estimation. In this case, $I_{REF} = M$.

The **Scale 1–3** experiments served to 1) train or retrain O's on the basic procedure of magnitude estimation and 2) investigate the nature of the ψ versus I relationship with different current ranges and reference currents. The third and fourth sessions were structured so that each of the experiments **MagIPI, MagNPB, MagPRR,** and **MagW** had an equal chance of appearing as the second or third experiment in the third or fourth session. Appendix A describes all of the ten experiments in detail.

Results

In several places we present only average data for six to seven observers. Full details, including a discussion of the effects of NPB, PRR, W, and IPI on S and M are in [22]. Appendix B provides details of the data analysis and statistical methods.

Magnitude Scales

Scale 1: Fig. 4 shows the relationship between $\overline{\psi}.(I)$ (mean of five replications) and I for the seven chosen O's who performed **Scale 1** (the results from the other three O's were similar but less repeatable). With individual variations, this relationship is an approximately linear function rather than a power function. The current scale is normalized so that 0 represents the sensation threshold S and 1 represents the maximal current without discomfort M.

Scale 2 explores the upper range of the ψ versus I relationship in more detail; eleven current levels span the upper half of the range from sensation threshold current S to maximal current without discomfort M. The many closely-spaced currents increase O confusion at midrange levels [22]. Again, however, the ψ estimates near $\psi(I_{REF})$ are reliable. **Scale 2** places $I_{REF} < M$ to extend the useful artifact-free range of the magnitude scale. Some O's were initially reluctant to specify test stimulus magnitudes above $\psi = 20$; they mistakenly identified $\psi(I_{REF}) = 20$ as $\psi(M)$. A simple verbal clarification and one repeat of the experiment corrected this situation.

Scale 3: Except for O1, the seven O's each completed **Scale 3** twice; the results are called **Scale 3a** and **Scale 3b.** The artifact-free range of $\psi(I)$ is the upper 40% of the I scale for most O's [22].

Averages: Fig. 5 shows the mean ψ of all seven O's for the four sessions of magnitude scale experiments. To facilitate comparison of the three different experiments, the current scale is normalized differently so that 0 represents sensation threshold current S and 1 represents the reference current I_{REF}, regardless of M. The $\psi(I)$ function is similar for all of the experiments. In particular, the individual nonmonotonicities disappear in the mean, suggesting that there is no systematic error in the scale for this group of O's. Also note the expected, slightly higher, slope for the **Scale 2** experiment because of its closely-spaced currents [23]. Finally, Fig. 6 shows that the mean of the SE's for all seven O's is minimized near the standard magnitudes (0 and 20). This supports the earlier assumption that magnitude estimation is easier near the standard levels.

MagNPBscreen

Fig. 7 shows Γ(NPB) for the seven selected O's (the results from the other three O's were more scattered, but similar in shape). All O's but O3 show a low Γ at low levels of NPB, confirming earlier results. O3 continued as an O because the small Γ variations were statistically significant ($p < 0.05$). Table I shows the mean over all

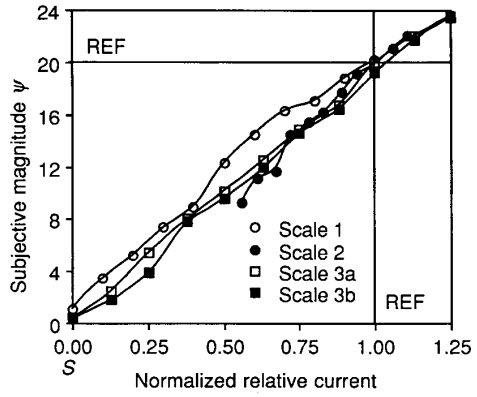

Fig. 5. The average magnitude versus current relationship for all observers is nearly linear regardless of current range or reference current (**Scale 1, 2, 3a, 3b**). This current scale is normalized so that the reference current is 1.

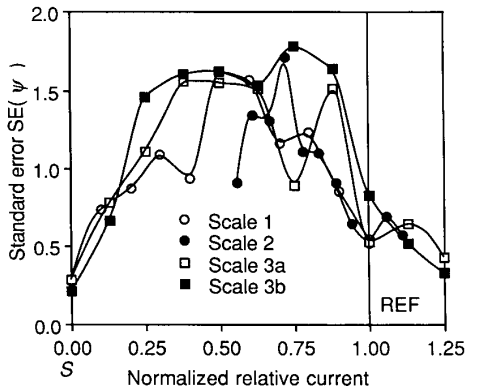

Fig. 6. The error in estimating magnitude is minimized near sensation threshold and reference level (**Scale 1, 2, 3a, 3b**).

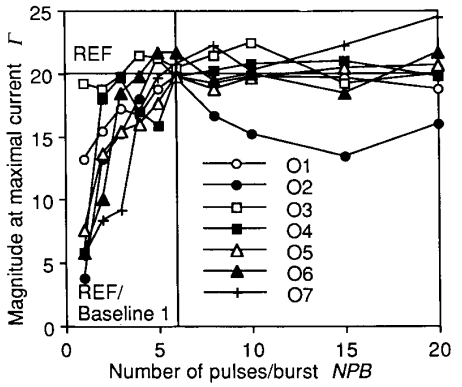

Fig. 7. **MagNPBscreen** screened observers by verifying that they could reliably detect the large increase in dynamic range Γ with increasing NPB. Three observers with similar but more scattered results are not shown.

waveforms w of the standard error SE($\bar{\Gamma}$.) for all of the **Mag** experiments and for **Search.**

Gradient and Search: Finding Baseline 2 Optimum

Table II shows the effects of the four waveform variables for the factorial experiment **Gradient** where a_1–a_4 are the single-variable effects for NPB, PRR, W, and IPI, respectively. For example, the single-variable effect a_1 is the change in Γ caused by increasing NPB from its lower value of four pulses/burst to its upper value of eight pulses/burst (Appendix A). These effects, along with the mean Γ of all conditions (a_0) and the variable interaction effects (changes in Γ that result only from changing two or more variables at a time), form a model that exactly describes the observed mean responses in the four-dimensional experiment (Appendix A).

The large-type entries in Table II shows the variable effects that exceed 2·SE(a), i.e., have less than 5%

TABLE I
MEAN VALUES OF SENSATION THRESHOLD CURRENT S AND MAXIMAL CURRENT WITHOUT DISCOMFORT M. DRIFT OF S AND M OVER 30 TRIALS. STANDARD ERRORS OF MEANS $\bar{S}.(w)$, $\bar{M}.(w)$, $\bar{\Re}.(w)$, AND $\bar{\Gamma}.(w)$ (REPLICATION ERROR).

Experiment	Observer	Mean $\bar{S}.(w)$ (mA)	Mean $\bar{M}.(w)$ (mA)	S Drift (%)	M Drift (%)	SE $\bar{S}.(w)$	SE $\bar{M}.(w)$	SE $\bar{\Re}.(w)$	SE $\bar{\Gamma}.(w)$
MagNPB screen	O1	1.85	5.72	6.3	25.1	0.066	0.15	0.13	0.92
	O2	1.72	3.80	11.7	−5.5	0.044	0.18	0.11	4.67
	O3	1.43	5.38	3.8	15.7	0.031	0.13	0.12	0.80
	O4	0.98	5.59	−2.9	33.0	0.087	0.65	1.19	1.76
	O5	1.14	7.35	−4.7	4.7	0.029	0.28	0.29	1.32
	O6	3.80	16.40	−3.3	7.5	0.082	0.31	0.12	0.73
	O7	1.97	4.83	2.8	34.9	0.106	0.15	0.15	1.42
Search	O1	1.82	8.74	6.9	27.0	0.056	0.35	0.24	0.83
	O2	1.51	3.17	−4.7	15.4	0.061	0.10	0.11	2.23
	O3	1.10	3.30	3.3	18.2	0.032	0.22	0.22	1.63
	O4	1.34	3.45	8.8	22.0	0.055	0.11	0.11	0.90
	O5	1.63	5.85	−6.9	24.3	0.099	0.27	0.27	1.32
	O6	2.25	14.55	8.6	12.4	0.060	0.13	0.18	0.40
	O7	3.05	8.39	−10.9	33.7	0.118	0.43	0.17	0.82
MagNPB	O1	—	—	—	—	—	—	—	—
	O2	1.56	2.89	−3.0	−7.2	0.086	0.10	0.11	3.84
	O3	1.22	5.51	9.3	37.0	0.033	0.30	0.28	1.29
	O4	1.97	8.21	7.9	83.5	0.027	0.29	0.15	0.69
	O5	1.73	8.01	−3.6	−0.4	0.040	0.20	0.16	1.58
	O6	1.76	9.72	4.9	22.9	0.049	0.35	0.25	0.59
	O7	2.06	4.66	−5.3	23.0	0.076	0.14	0.10	1.17
MagPRR	O1	—	—	—	—	—	—	—	—
	O2	3.00	5.60	−12.3	3.4	0.099	0.12	0.08	1.70
	O3	1.65	4.69	0.0	12.8	0.020	0.10	0.07	0.39
	O4	2.05	6.78	10.0	14.0	0.069	0.20	0.16	0.31
	O5	1.67	8.50	−5.6	8.8	0.018	0.16	0.11	0.72
	O6	2.46	12.18	−10.1	26.4	0.126	0.26	0.30	0.43
	O7	1.82	7.27	46.8	38.4	0.237	0.33	0.52	0.92
MagW	O1	1.63	5.54	0.9	0.3	0.022	0.19	0.12	0.51
	O2	1.28	2.81	0.4	−5.3	0.013	0.15	0.10	2.87
	O3	1.30	5.72	4.6	23.0	0.040	0.37	0.27	1.40
	O4	2.46	6.35	10.7	37.2	0.067	0.32	0.16	1.18
	O5	1.55	7.48	−0.8	18.1	0.041	0.30	0.19	2.26
	O6	2.57	12.60	11.8	7.9	0.112	0.22	0.22	0.50
	O7	0.97	6.60	−4.0	51.3	0.064	0.34	0.60	1.46
MagIPI	O1	1.59	7.06	−1.0	13.8	0.017	0.14	0.10	0.42
	O2	3.21	5.19	20.8	8.3	0.120	0.15	0.08	2.22
	O3	1.54	4.90	4.4	29.5	0.033	0.16	0.13	0.49
	O4	2.25	6.43	25.0	10.5	0.122	0.22	0.20	0.92
	O5	1.82	8.74	−3.7	7.1	0.038	0.17	0.13	0.70
	O6	1.80	9.79	−2.6	6.3	0.033	0.43	0.26	0.66
	O7	2.81	5.00	34.3	35.4	0.086	0.21	0.09	1.04

TABLE II
VARIABLE EFFECTS FOR GRADIENT EXPERIMENT. LARGE TYPE DENOTES EFFECTS $a \geq 2 \cdot \mathrm{SE}(a)$, i.e., $p \leq 0.05$

Effect	O1	O2	O3	O4	O5	O6	O7
a_1 (*NPB*)	−0.57	0.85	−0.27	**0.82**	0.93	**2.33**	**0.93**
a_2 (*PRR*)	−0.43	0.40	**1.22**	0.33	**2.33**	0.43	−0.48
a_3 (*W*)	−0.07	**3.75**	**0.97**	**1.53**	−0.58	0.38	0.32
a_4 (*IPI*)	−0.13	0.45	−0.58	0.22	0.47	−0.27	−0.07
a_{12}	−1.17	**2.55**	0.83	**−0.58**	−0.27	0.47	0.37
a_{13}	−0.33	1.10	−0.23	0.22	−0.47	−0.28	0.48
a_{14}	−0.08	−0.60	0.32	0.13	−1.03	−0.23	0.58
a_{23}	0.62	−0.95	−0.32	0.73	−0.47	0.33	0.27
a_{24}	**1.28**	**1.35**	0.22	0.12	0.18	**0.57**	0.68
a_{34}	0.92	0.60	0.77	−0.28	−0.43	**1.03**	−0.53
a_{123}	−0.33	**−2.20**	−0.33	**−0.77**	0.72	**−0.92**	0.12
a_{124}	−0.18	0.70	−0.47	0.02	0.38	0.43	−0.57
a_{134}	**−1.63**	−1.25	0.28	**−0.58**	**2.68**	−0.13	0.12
a_{234}	−0.47	−0.30	−0.63	−0.17	−0.13	−0.02	**−0.98**
a_{1234}	−0.32	−2.15	−0.13	0.33	−1.93	0.33	0.58
a_0 (Mean)	20.84	17.05	19.56	19.36	20.01	19.84	20.09
SE(a)	0.64	1.15	0.46	0.26	1.00	0.24	0.40
scale	0.22	0.15	0.25	0.25	0.20	0.13	0.15

chance of occurring due to closeup error. While effects due to NPB, PRR, and W usually dominate, two and three-factor interactions are present, suggesting a complex response surface. Such strong interactions could potentially undermine the gradient search for the maximal Γ.

We found out that this was not the case, although the response for $\Gamma(k)$ was somewhat scattered. Fig. 8 shows Γ along the gradient path [Fig. 3 and (A2)] for each O who completed **Search.** A second-order polynomial fit for each O's data shows that Γ increases and peaks at $3 \leq k \leq 10$, confirming the correct gradient direction for all but O4. However, rather than using the peak of this polynomial model, we used the value of k that maximized the actual data Γ to determine the new optimal w. *Baseline 2* (F = 15 Hz, NPB = 7, PRR = 400 Hz, W = 120 μs, and IPI = 100 μs) is approximately the mean of the waveform variable values that maximized Γ for each of the 7 O's.

Single-Variable Effects

Figs. 9–12 respectively show how $\bar{\Gamma}_{\cdot}$ varies with the 10 levels of the scalar independent variables NPB, PBR, W, and IPI for each of the seven O's. Figs. 1/3–1/6 show the mean $\bar{\Gamma}_{\cdot,\cdot}(k)$ and the geometric mean $\Re_{\cdot,\cdot}(k)$ over all 6 or 7 O's (O1 did not complete **MagNPB** or **MagPRR**) The error bars show the standard error (SE) of the mean. Finally, Table III shows the p-values from the ANOVA test for each O performing each of the four single-variable experiments. These results are not without bias. O's with low overall M/S ratios (e.g., O2 in Table I) tend to show high (insignificant) p-values because the narrow current range causes small errors in determining M to translate into large effective errors in Γ by (B5)—a narrow current range necessarily expands the magnitude scale to fit the current scale. Some O's (e.g., O3 in Figs. 9–12) have low p-values because they do not show strong reactions to different waveforms for any experiment. Conversely, some very experienced observers, (e.g., O6) can easily distinguish between waveforms even when presented in different random orders, leading to several highly significant effects. We will therefore concentrate on the mean plots in Figs. 13–16 rather than on the statistical results.

MagNPB: Figs. 9 and 13 and Table I show that the increase in Γ with increasing NPB is clearly the most important effect. The large increase in Γ is not accompanied by a corresponding increase in $\Re$. In fact, the maximal value of $\Re$ occurs at NPB = 2, far from providing the most intense comfortable stimulus (NPB = 6).

MagPRR: Fig. 14 shows that PRR has little consistent effect on Γ or $\Re$. The observed effects are likely due more to changes in percept *quality* than magnitude. One O who in an informal experiment continuously varied PRR noted that for high values of PRR (>700 Hz), the percept was more vibratory in nature (desirable), but stinging sensations occurred at lower vibratory magnitudes (undesirable) than at lower PRR. This is consistent with [12]. Lower values of PRR (<350 Hz) produced a percept of "higher frequency," and the six O's interpreted this differently (Fig. 10).

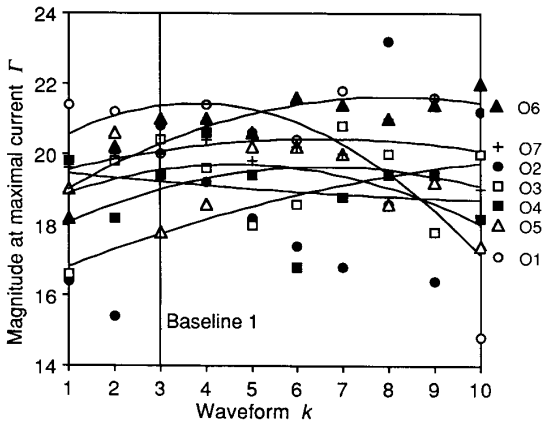

Fig. 8. **Search:** The dynamic range Γ typically increases, peaks, and then decreases as the waveform w advances along the gradient $\nabla\Gamma(w)$. A second-order polynomial fit (curved lines) shows this more clearly than the raw data.

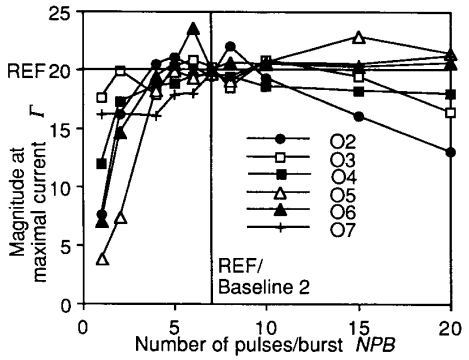

Fig. 9. **MagNPB:** Dynamic range increases greatly from NPB = 1 to NPB = 6 for most observers.

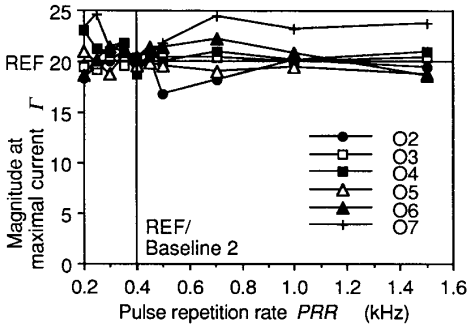

Fig. 10. **MagPRR:** Dynamic range changes differently with PRR for different observers.

The sharp dip at PRR = 400 Hz for most O's may be caused by the reference stimulus having the same PRR; the O's may note that the reference and test waveform qualities are similar and thus bias their magnitude estimates. This is supported by the low spread in magnitude estimates at 400 Hz compared to other values of PRR. We conclude that any PRR value between 200 and 800 Hz is Suitable; different O's may prefer different values. The

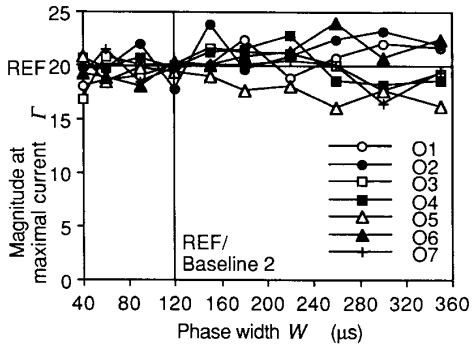

Fig. 11. **MagW:** Dynamic range increases with W for some observers and decreases for others, suggesting two groups of skin stimulation sites.

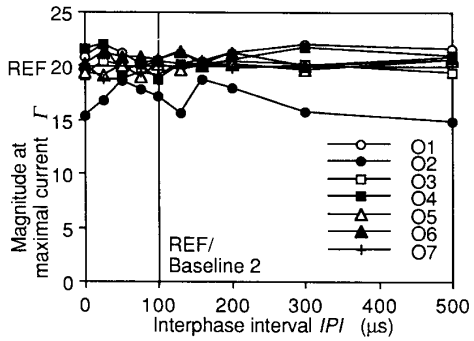

Fig. 12. **MagIPI:** Dynamic range does not change with IPI. O2's unrepresentative large variations are not statistically significant due to large experimental error (Table I).

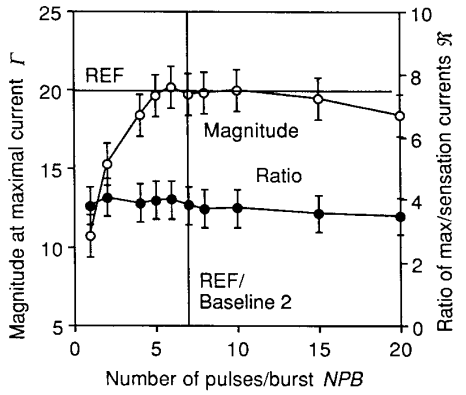

Fig. 13. The average dynamic range for six observers is maximized when NPB = 6 (**MagNPB**). The ratio ℜ of maximal current without discomfort to sensation threshold current is maximized when the magnitude dynamic range is low.

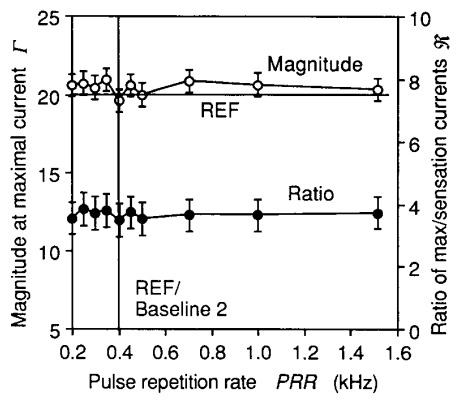

Fig. 14. The average dynamic range for six observers is maximized when PRR = 350 Hz, but the effect is small (**MagPRR**).

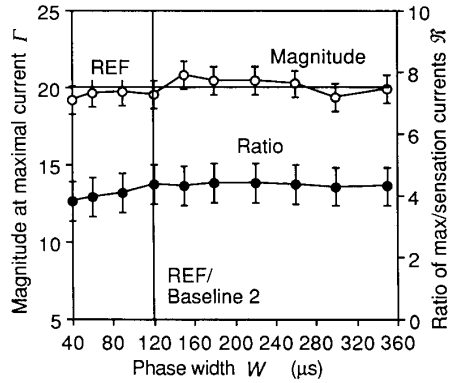

Fig. 15. The average dynamic range for seven observers is maximized when W = 150 μs, but the effect is small (**MagW**).

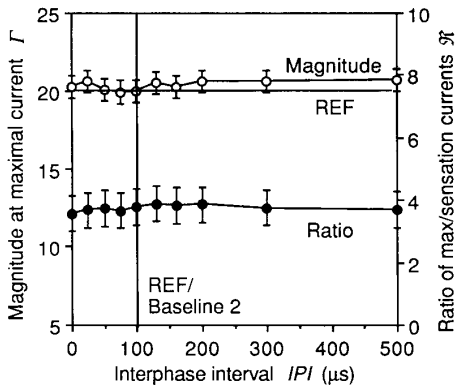

Fig. 16. The average dynamic range for seven observers is not affected by IPI (**MagIPI**). Error bars show SE (mean).

average $\bar{\Gamma}_{..}$(PRR) is maximized by PRR = 350 Hz (Fig. 14).

MagW: The small effect of phase width W on Γ separates the O's into two groups. Fig. 11 shows that for O1, O2, and O6, Γ increases with W whereas for O3, O4, O5, and O7, Γ decreases with W. Because we did not repeat this experiment at different skin locations on the same O, this effect may rather represent two groups of skin sites with different tactile afferent innervations, because shifts of electrode position as small as 1 mm can result in different electrotactile percepts [1]. The mean Γ for all seven O's (Fig. 15) peaks at W = 150 μs, but values between 150 and 260 μs result in a similar Γ. ℜ increases slightly with W up to 220 μs and then falls, approximately following the variation in Γ. Both ℜ and Γ continue to fall at increasing values of W; the uncomfortable stinging sen-

TABLE III
ANOVA p-VALUES FOR **MagNPB, MagPRR, MagW,** AND **MagIPI** EXPERIMENTS. LARGE TYPE DENOTES $p \leq 0.05$.

Indep. Var.	Expt.	O1	O2	O3	O4	O5	O6	O7
$\mathfrak{R}$	*NPB*	—	0.376	**0.005**	0.087	0.226	**0.028**	0.072
$\mathfrak{R}$	*PRR*	—	0.218	0.342	**0.020**	0.843	0.499	0.661
$\mathfrak{R}$	*W*	**0.000**	**0.000**	0.759	0.283	0.302	**0.018**	0.458
$\mathfrak{R}$	*IPI*	**0.019**	0.597	0.536	0.734	0.108	0.828	0.412
Γ	*NPB*	—	0.283	0.265	**0.000**	**0.000**	**0.000**	**0.026**
Γ	*PRR*	—	0.828	0.121	**0.000**	0.471	**0.000**	**0.011**
Γ	*W*	**0.000**	0.903	0.322	0.208	0.884	**0.000**	0.582
Γ	*IPI*	0.066	0.915	0.661	0.297	0.843	0.850	0.903

sation produced by waveforms with $W > 500$ μs is well-known [15], [24], [25]. We did not explore the region $W < 10$ μs where $\mathfrak{R}$ is reported to decrease substantially [26].

MagIPI: Interphase interval IPI has no apparent effect on $\mathfrak{R}$ or Γ. Fig. 12 shows no consistent changes in Γ with IPI; the relatively large effect in O2's data is not statistically significant ($p > 0.05$) due to the large error. O2's unrepresentative data are not included in the mean $\overline{\Gamma}_{.,.}$(IPI) or $\overline{\mathfrak{R}}_{.,.}$(IPI) plots (Fig. 16).

DISCUSSION

Magnitude Scale

The maximization of magnitude dynamic range depends only on a relatively smooth and monotonic relationship between the stimulus current I and the corresponding perceived magnitude ψ in the upper region of the function near the maximal magnitude without discomfort Γ. While no particular function is necessary, our magnitude-estimation method reduces the error in estimating ψ near Γ and also provides a convenient method to estimate cumulative magnitude-estimation errors in the two-stage optimization experiments (Appendix B).

The resulting linear magnitude scale is not "pure" because standard levels are defined: $\psi(S) = 0$ (sensation threshold) and $\psi(I_{\mathrm{REF}}) = 20$ (reference). The experiment therefore more closely defines a category scale than a true magnitude scale [23], [27]. We chose this method in spite of its limitations [27], [28] because in the optimization experiments we require O to make fine distinctions in magnitude near a reference magnitude. The result is that the magnitude versus current function is approximately linear rather than the usual power function [14]–[16]. While inflating error in other regions of the magnitude scale, presenting the reference stimulus reduces the error near $\psi(I_{\mathrm{REF}})$, the region of interest for optimizing the dynamic range.

The data frequently show a nonuniformity in O's use of the magnitude scale (Fig. 4). In particular, some O's (O1, O5, and O6) tended to cluster magnitude estimates near the REF level, causing a lower slope in this region. Other O's (O4, O7) showed a similar preference for the lower end of the scale. These end effects are expected because the magnitude is easier to estimate near the standard levels than in the middle of the scale [23].

Occasionally, the ψ versus I relationship is nonmonotonic in one or more regions. This effect is not likely artifactual; it frequently exceeds the standard error of the magnitude estimations, and it occurs in three O's (O2, O4, and O7). One possible explanation is that O mentally constructs two (or more) different scales depending on the approximate magnitude of the test stimulus. Low-level stimuli are therefore compared to zero, and high-level stimuli are compared to the REF stimulus. The two scales may not coincide at intermediate levels, causing confusion and inaccurate magnitude estimations. Fortunately, because the dynamic range optimization experiments present stimuli mostly near the reference level, this occasional nonmonotonicity should not bias the optimization results.

Optimal Waveform

We speculate that the large Γ increase from NPB = 1 to NPB = 6 may be due to an increased proportion of afferent touch (α) fibers being stimulated by the repetitive pulses compared with the pain (γ) fibers. Considering that PRR = 350 Hz, this is consistent with the high sensitivity of normal touch to vibration in the 100–600 Hz range [29].

The drop in Γ at higher NPB may be attributable to a change in percept quality; the stimulation at NPB $\geq$ 15 feels higher in "frequency" than stimulation at lower NPB. While O's might be expected to interpret this percept as stronger than one that feels lower in frequency [30], it takes on a character more of pressure than vibration. Some O's noted that such variations in percept quality between trials made magnitude comparisons difficult. This higher-frequency percept is expected because long bursts span a large portion of the overall waveform period T, and therefore the waveform begins to look like a continuous train of pulses at a high frequency. (The definitions of the waveform variables allow for this redundancy. For example, a waveform defined by W = IPI = 50 μs, NPB = 1, F = 400 Hz is identical to a waveform with W = IPI = 50 μs, NPB = 10, F = 40 Hz, PRR = 400 Hz.)

Finally, increasing NPB from 1 to 6 caused the average charge/burst delivered to the skin to increase from 2.11 to 7.14 μC for a fixed percept magnitude $\psi = \Gamma$(NPB = 1). The highest possible magnitude Γ(NPB = 6) required 10.9 μC. Furthermore, this increased charge might be expected to cause increased skin irritation and sensory adaptation.

These experiments support the recommendations of other investigators to deliver repeating bursts of stimulation pulses: (functionally monophasic, F = 25 Hz, NPB = 4, PRR = 500 Hz, W = 20 μs) in [26], [31]; (balanced-biphasic, F = 100–250 Hz, NPB = 1–40, PRR = 10 kHz, W = 5–20 μs, IPI = 5–25 μs) in [12], [13], [32]; (balanced-biphasic, F = 30 Hz, NPB = 1–150, PRR = 10 kHz, W = 4.5–9 μs, IPI = 41–45.5 μs) in [17].

CONCLUSIONS

The sensation produced by electrotactile stimulation has comfortable (vibratory) and uncomfortable (stinging) percepts. The maximal-acceptable level of the stinging per-

cept limits the stimulation current and hence the useful dynamic range.

A waveform with the number of pulses/burst NPB = 6, pulse repetition rate PRR = 350 Hz, and phase width W = 150 μs maximizes the intensity (magnitude) of the vibratory percept compared with the stinging percept. In particular, waveforms with fewer pulses/burst substantially reduce the intensity of the vibratory percept (50% reduction at NPB = 1) while largely maintaining the sting. The interphase interval IPI between positive and negative phases of a balanced-biphasic waveform has no effect on dynamic range.

These experiments maximized the electrotactile dynamic range for one electrode geometry (5.5-mm-diameter-active coaxial) at one skin site (abdomen) with the balanced-biphasic pulse bursts delivered at one rate (15 Hz). The effects of W and PRR may be dependent on skin site or observer. Furthermore, only one electrode delivered stimulation; the effects of spatial integration and masking may alter the optimal waveform for multiple-electrode arrays.

Measuring stimulation intensity at a predetermined maximal current without discomfort (for each waveform) provides a measure of electrotactile intensity dynamic range that is more relevant to the overall comfort of the stimulation percept than the ratio of pain threshold to sensation threshold. In most cases, the two measures yield different information.

Appendix A
Detailed Experiment Descriptions

Scale 1: Magnitude Scale

Choice of Stimulation Waveform and Current: Based on preliminary unpublished data from four O's, the waveform variables for **Scale 1** were fixed at *Baseline 1* (F = 15 Hz, PRR = 400 Hz, W = IPI = 100 μs, and NPB = 6), which was the first approximation of the waveform $\boldsymbol{w}$ that maximizes $\Gamma(\boldsymbol{w})$. O first determined the sensation threshold current S by a modified method of limits. Upon prompt by the computer, O turned a knob CW, starting at the zero (fully CCW) position, until s/he perceived a distinct but very weak tingling sensation at the electrode site. We instructed O to readjust the knob CW and CCW until s/he could just barely feel the stimulus, and then press the ENTER (RETURN) key on the keyboard, causing S to be logged to a result file and saved in memory for future use. Then O returned the knob to zero. This procedure was then repeated two more times. The computed averaged the three results to obtain

$$\bar{S}. = (S_1 + S_2 + S_3)/3.$$

Next, O determined the maximal current without discomfort M. Starting at zero, O turned the knob CW until the stimulus was as strong as possible without feeling uncomfortable as manifest by sharp, prickly, or burning sensations. O logged the response by pressing ENTER and then returned the knob to zero. As for the sensation threshold, the computer calculated the mean $\bar{M}.$ of three trials. A 10-s separation between M trials allowed O's somatosensory system to partially recover from sensory adaptation.

Finally, the computer calculated the set of eleven test-stimulus currents (independent variable) for magnitude estimation, as well as a reference-stimulus current:

$$I_0 = \bar{S}. + 0.00(\bar{M}. - \bar{S}.) = \bar{S}.$$

$$I_1 = \bar{S}. + 0.10(\bar{M}. - \bar{S}.)$$

$$I_2 = \bar{S}. + 0.20(\bar{M}. - \bar{S}.)$$

$$\vdots$$

$$I_{10} = \bar{S}. + 1.00(\bar{M}. - \bar{S}.) = \bar{M}.$$

$$I_{\text{REF}} = I_{10}$$

Magnitude Estimation: We then asked O to rate these eleven stimulus currents numerically on an magnitude scale where:

Level 0 = Cannot feel test stimulus.
Level 1 = Can barely feel test stimulus.
Level 20 = Test stimulus same magnitude as reference REF.

Open-ended upper scale; assign numbers as appropriate.

The computer presented the reference stimulus before each test stimulus (same electrode) so that O did not need to remember the REF magnitude for more than 2 s. Earlier unpublished experiments on four O's with the reference presented less frequently (e.g., once every ten trials) showed that their magnitude estimations tended to drift substantially upward or downward (sometimes even reversing direction midway) between reference presentations.

O reviewed the magnitude estimation instructions on the computer screen (previously given verbally). The computer then presented five sets (replications) of eleven magnitude estimation trials at the levels I_0–I_{10}. Each replication r presented the trials in a different computer-generated random order [19]. Each trial consisted of these actions:

1) Computer gives beep sound, gives message on screen that next stimulus is coming, then pauses for 6 s.
2) Beep, message READY!, then a 1-s pause.
3) Beep, computer delivers a 1-s reference stimulus with current I_{REF} (level 20).
4) Beep, computer delivers a 1-s test stimulus at one of the eleven currents I_0–I_{10}.
5) Beep-beep, computer prompts O to type in a number representing the magnitude $\psi_{rj}(I)$ of the test stimulus.

Scale 2: Magnitude Scale

Scale 2 was similar to **Scale 1** except that a smaller range of currents was tested to provide more detail in the

magnitude region of interest (near the maximal magnitude without discomfort). Also, the reference current was lowered to $0.9 \cdot M$ to expand the low-error region of ψ near the reference magnitude:

$$I_0 = \bar{S}_\cdot + 0.50(\bar{M}_\cdot - \bar{S}_\cdot) = \bar{S}_\cdot$$
$$I_1 = \bar{S}_\cdot + 0.55(\bar{M}_\cdot - \bar{S}_\cdot)$$
$$I_2 = \bar{S}_\cdot + 0.60(\bar{M}_\cdot - \bar{S}_\cdot)$$
$$\vdots$$
$$I_{10} = \bar{S}_\cdot + 1.00(\bar{M}_\cdot - \bar{S}_\cdot) = \bar{M}_\cdot$$
$$I_{\text{REF}} = I_8$$

Scale 3: Magnitude Scale

Scale 3 was identical to **Scale 1** except that the reference current was $0.8 \cdot M$ to further expand the low-error region:

$$I_0 = \bar{S}_\cdot + 0.00(\bar{M}_\cdot - \bar{S}_\cdot) = \bar{S}_\cdot$$
$$I_1 = \bar{S}_\cdot + 0.10(\bar{M}_\cdot - \bar{S}_\cdot)$$
$$I_2 = \bar{S}_\cdot + 0.20(\bar{M}_\cdot - \bar{S}_\cdot)$$
$$\vdots$$
$$I_{10} = \bar{S}_\cdot + 1.00(\bar{M}_\cdot - \bar{S}_\cdot) = \bar{M}_\cdot$$
$$I_{\text{REF}} = I_8$$

The waveforms were at *Baseline 2* (F = 15 Hz, PRR = 400 Hz, W = 120 μs, IPI = 100 μs, and NPB = 7).

MagNPBscreen: Effect of NPB

Earlier unpublished results (four O's) showed a large predictable increase in Γ as NPB increased from 1 to 10. We therefore screened O's ability to discern this change. All waveform variables were fixed at *Baseline 1* except for the independent variable NPB, which had values NPB_1, NPB_2, $\cdots$ NPB_{10} of 1, 2, 3, 4, 5, 6, 8, 10, 15, and 20 pulses/burst.

Sensation Threshold Current: First, O determined the sensation threshold current $S_{uj}(\text{NPB})$ using the procedure in **Scale 1** for each of the ten values of NPB. Three replications u of these ten trials were performed in different random orders. The index j specifies the actual run order (trial) within each replication.

Maximal Current without Discomfort: Next, O determined the maximal current without discomfort $M_{vj}(\text{NPB})$ using the procedure in **Scale 1** for each of the ten values of NPB (three replications v). Possibly because the 10-s interval between M trials provides insufficient time for the skin to completely recover from sensory adaptation, the 30 values for M usually show a distinct upward trend (Fig. 17). (In rare cases, it is downward, usually indicating insufficient skin hydration or poor electrode-skin contact.) This drift averaged 19% over the 30 trials, lying between 0.3 and 30% for 80% of the experiments (Table I). The drift systematically increases the replication variance

$$\frac{1}{V-1}\sum_{v=1}^{V}[M_{vj}(\boldsymbol{w}) - \bar{M}_{\cdot j}(\boldsymbol{w})]^2$$

in determining M at each level of NPB (V = 3). Because the drift is monotonic and approximately linear, we compensate by subtracting a correction factor from each logged current M (in effect, removing a linear approximation of the drift):

$$M'_{vj}(\boldsymbol{w}) = M_{vj}(\boldsymbol{w}) - b(j' - 15) \quad \text{where}$$
$$j' = j + 10(v - 1) \quad \text{and}$$
$$b = [\bar{M}_{3\cdot}(\cdot) - \bar{M}_{1\cdot}(\cdot)]/20 \quad \text{and} \qquad \text{(A1)}$$

M' is the corrected current M, v is the replication (1 . . . V = 3), j is the trial in each replication (1 . . . 10 corresponding to the ten values of NPB in random order), j' is the sequence of all trials in the three replications (monotonic with time), $\bar{M}_{3\cdot}$ and $\bar{M}_{1\cdot}$ are the means of all maximal currents in replications 3 and 1, respectively, and b is the estimated slope of the drift (mA/trial). The method of using the replication means $\bar{M}_{3\cdot}$ and $\bar{M}_{1\cdot}$ results in a slope b similar to that obtained by a linear regression of M_{vj} versus j', but it has less bias due to the effect of NPB on M because $\bar{M}_{3\cdot}$ and $\bar{M}_{1\cdot}$ are means over all ten values of NPB. Any residual effect of the nonlinear part of the drift is reflected in the calculated replication variance and is random because the trials determining M were performed in random order.

It is well-known that O training increases M [3], [13], [33]. However, all of these experiments are within-O designs (each O receives all treatments) so that differences in O experience are not likely to systematically bias the results.

The computer then calculated the mean drift-corrected currents $\bar{M}'_\cdot(\text{NPB}_1)$, $\bar{M}'_\cdot(\text{NPB}_2)$, . . . $\bar{M}'_\cdot(\text{NPB}_{10})$ for presentation to O. Furthermore, $\text{NPB}_{\text{REF}} = \text{NPB}_5 = 6$ pulses/burst with associated current $I_{\text{REF}} = \bar{M}'_\cdot(\text{NPB}_5)$ was also used as the reference stimulus. Finally, a lower-current stimulus

$$I_{\text{LOW}} = \bar{S}_\cdot(\text{NPB}_{\text{REF}}) + 0.75[\bar{M}'_\cdot(\text{NPB}_{\text{REF}}) - \bar{S}_\cdot(\text{NPB}_{\text{REF}})]$$

provided a scaled relating a change in current ΔI to a change in magnitude $\Delta\psi$ so that error in determining M could be related to the resulting error in ψ and hence Γ.

Magnitude Estimation: We then asked O to rate these ten waveforms (with NPB_1, NPB_2, . . . NPB_{10}) numerically on a magnitude scale using the procedure from **Scale 1.** The computer presented five replications of ten magnitude estimation trials. Each replication r presented the ten trials $\Gamma_r(\text{NPB}_1) - \Gamma_r(\text{NPB}_{10})$ in a different random order. Interspersed in each replication were two magnitude estimations of the REF current $\psi_r(11)$, $\psi_r(12)$ and two magnitude estimations of the LOW current $\psi_r(13)$, $\psi_r(14)$.

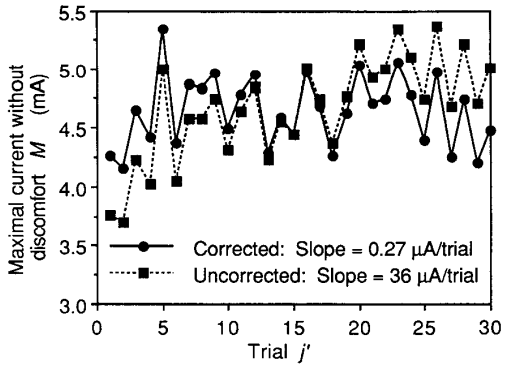

Fig. 17. A linear correction compensates for the typical upward drift in the maximal current without discomfort M with time. Trials are monotonic with time. (Data from experiment **MagNPB**, observer O7).

Observer Screening

We reviewed data from the session 1 (**Scale 1** and **MagNPBscreen** experiments) before proceeding with sessions 2–4 to make sure that O understood the procedures. Three of the ten O's initially contacted were dismissed at this point because graphs their magnitude estimates were very jagged, scattered and unrepeatable, although similar in trend to the smoother results of the chosen O's. We speculate that this scatter was caused by lack of O's attention to the task.

Gradient: Determination of Gradient and Interactions

Independent Variables: Earlier unpublished results suggested that the effects of the waveform variables F, NPB, PRR, W, and IPI strongly interacted, i.e., the effect of one variable depended on the values of one or more of the others [34]. Therefore, we conducted a full factorial experiment in NPB, PRR, W, and IPI to (1) evaluate the effects of such interactions, and (2) determine the gradient of the response surface $\nabla\Gamma$(NPB, PRR, W, IPI), i.e., the vector that points in the direction of increasing Γ. Knowing the gradient provides an efficient method to simultaneously vary (NPB, PRR, W, IPI) to search for the waveform variables that maximize Γ.

Fixed Variable: Because F has a direct effect on ψ [30], O's had a difficult time separating changes in Γ from changes in the perceived frequency. Therefore, F remained constant at 15 Hz for these experiments. Higher frequencies cause increasingly rapid sensory adaptation; lower frequencies result in a low communication rate as evidenced by a noticeable lag between stimulus magnitude and attempted magnitude changes with the knob during determination of S and M.

Factorial Structure: The computer administered the three-stage experiment (S, M, Γ) as in **MagNPBscreen,** but with the variable settings in Table IV. These settings form an orthogonal experiment which simplifies calculation of the variable effects and the gradient [34]. Waveform conditions 17 and 18 are the REF waveform (defined as the *Baseline 1* stimulus) located in the center of the hypercube formed by the set of all 16 points (NPB, PRR, W, IPI).

Threshold and Maximal Currents: To each of seven O's, the computer administered three replications u of sensation threshold current S and three replications v of maximal current without discomfort M determinations with the waveforms w in Table IV. As before, the computer corrected the M values for drift (A1) and then averaged three replications of M'.

Magnitude Estimation: The O's then estimated the magnitude of the 16 waveforms $\Gamma_r(w_1) - \Gamma_r(w_{16})$ plus two REF-current estimations $\psi_r(w_{17}) - \psi_r(w_{18})$ plus two LOW-current estimations $\psi_r(w_{19}) - \psi_r(w_{20})$. O performed five replications r of these 20 trials in different random orders.

Search: Find Maximal Γ Along Gradient Path

The gradient search is based on the linear approximation in the vicinity of the *Baseline 1* waveform w_{REF}

$$\Gamma(w) \approx \Gamma(w_{REF}) + a_1'(\text{NPB} - \text{NPB}_{REF}) + a_2'(\text{PRR} - \text{PRR}_{REF}) + a_3'(W - W_{REF}) + a_4'(\text{IPI} - \text{IPI}_{REF})$$

where the constants

$$a_1' = \frac{\partial\Gamma}{\partial\text{NPB}}(w_{REF})$$

$$a_2' = \frac{\partial\Gamma}{\partial\text{PRR}}(w_{REF})$$

$$a_3' = \frac{\partial\Gamma}{\partial\text{W}}(w_{REF})$$

$$a_4' = \frac{\partial\Gamma}{\partial\text{IPI}}(w_{REF})$$

define a least-squares regression. In practice, we estimated these coefficients by scaling the main (single-factor) effects $a_1 - a_4$ (calculated in the effects analysis in the "Results" section).

Before proceeding with each O, we calculated the gradient $\nabla\Gamma(w)$ separately for each O based on the **Gradient** experiment:

$$\nabla\Gamma(w) = \begin{bmatrix} a_1 \\ a_2 \\ a_3 \\ a_4 \end{bmatrix}$$

The path of steepest ascent (i.e., the direction in w that most quickly increases Γ) is then (Fig. 3)

$$\text{NPB}(k) = \text{NPB}_{REF} + a_1 \cdot scale \cdot (k - 3)$$

$$\text{PRR}(k) = \text{PRR}_{REF} + a_2 \cdot scale \cdot (k - 3)$$

TABLE IV
INDEPENDENT VARIABLE SETTINGS FOR **Gradient** EXPERIMENT

Waveform *w*	*NPB*	*PRR* (Hz)	*W* (μs)	*IPI* (μs)
1	4	300	75	75
2	8	300	75	75
3	4	500	75	75
4	8	500	75	75
5	4	300	125	75
6	8	300	125	75
7	4	500	125	75
8	8	500	125	75
9	4	300	75	125
10	8	300	75	125
11	4	500	75	125
12	8	500	75	125
13	4	300	125	125
14	8	300	125	125
15	4	500	125	125
16	8	500	125	125
17	6	400	100	100
18	6	400	100	100

$$W(k) = W_{REF} + a_3 \cdot scale \cdot (k - 3)$$

$$IPI(k) = IPI_{REF} + a_4 \cdot scale \cdot (k - 3) \qquad (A2)$$

where k is a scalar index between 1 and 10 (i.e., the waveform w) and *scale* is an arbitrary constant that specifies the size of the steps for the gradient search (Table II). To verify that the gradient direction was approximately correct, the gradient search was performed backwards ($k = 1 \ldots 2$) from *Baseline 1* ($k = 3$) as well as forwards ($k = 4 \ldots 10$). If the gradient direction is correct, Γ should increase as $k > 3$ and decrease as $k < 3$, at least in the region near *Baseline 1* where a linear approximation of Γ is valid. Eventually, as the linear approximation breaks down, Γ should peak and then decrease as k continues to increase. The waveform w corresponding to the value of k that maximized Γ, where w was averaged over all 7 O's, became the new optimum, *Baseline 2*.

MagNPB, MagPRR, MagW, and MagIPI: Single-Variable Effects

The same seven O's then proceeded with a set of experiments that varied one-at-a-time each of the four waveform variables NPB, PRR, W, and IPI around *Baseline 2*. Ten levels of the independent variable were presented for each experiment, using the three-step procedure in **MagNPBscreen** (determination of the sensation threshold current S, the maximal current without discomfort M, and the magnitude at maximal current without discomfort Γ). The independent variable levels were

NPB: 1, 2, 4, 5, 6, **7,** 8, 10, 15, 20 pulses/burst

PRR: 200, 250, 300, 350, **400,** 450, 500, 700, 1000, 1500 Hz

W: 40, 60, 90, **120,** 150, 180, 220, 260, 300, 350 μs

IPI: 0, 25, 50, 75, **100,** 130, 160, 200, 300, 500 μs

The boldface numbers along with the fixed value $F = 15$ Hz define the *Baseline 2* waveform, i.e., values for the waveform variables that were *not* varied in a particular experiment. *Baseline 2* was also used for the reference waveform. As above, the S and M determinations consisted of three replications of ten independent variable values, while the magnitude determinations consisted of five replications of ten independent variable values $\Gamma_{rj}(w_1) - \Gamma_{rj}(w_{10})$ plus two REF-current stimuli $\psi_{rj}(w_{11}) - \psi_{rj}(w_{12})$ plus two LOW-current stimuli $\psi_{rj}(w_{13}) - \psi_{rj}(w_{14})$ (all in different random orders).

APPENDIX B
DATA ANALYSIS

Data Correction

The tedious nature of these experiments caused some O's to lapse in concentration or enter magnitude estimates incorrectly, e.g., entering 9 instead of 19 on the keyboard. We manually scanned the data from each experiment for errors by comparing the five replications r of the magnitude estimation for each waveform w. If one entry was far different from the other four, we attempted to correct the assumed error under the following conditions: 1) The error must be obvious. For example, for a set of five replicated ψ values (19, 20, 10, 20, 20), the value 10 is very likely a misentry, whereas the data set (4, 16, 8, 13, 9) indicates genuine nonrepeatability, not simply careless entry. 2) There must be only one assumed errant entry in the five replicates. If the assumed error was attributable to a missed, extra, or adjacent keystroke we corrected the single keystroke. In the above example, we replaced 10 with 20. If the error appeared to be due to lapse of concentration, we replaced the assumed error with the closest integer mean of the other four points; e.g., (20, 6, 4, 9, 4) was changed to (6, 6, 4, 9, 4). We did not attempt to correct data that did not meet both conditions; doubtful data were unaltered. No single experiment required more than two corrections; 53 of the 67 experiments required no corrections.

Error Analysis

The calculations of variance and standard error of the mean (SE) for S and M are straightforward, as these measurements are replicated $U = V = 3$ times:

$$\text{Var}\,[M'_v(w)] = \frac{1}{V-1}\sum_{v=1}^{V}[M'_v(w) - \overline{M}'.(w)]^2$$

$$\text{SE}[\overline{M}'.(w)] = \sqrt{\frac{1}{V}\,\text{Var}\,[M'_v(w)]}$$

where M'_v is the drift-corrected M from (A1), v is the replicate, $M'.(w)$ is the mean of three replicates, and w is the waveform. (The calculations are identical for S).

The variance of $\overline{\mathfrak{R}}.(w)$ is approximated by the variance

of the first term of its Taylor Series expansion [35]:

$$\text{Var}\,[\overline{\Re}.(w)] = \left(\frac{\overline{\Re}.(w)}{\overline{M}'.(w)}\right)^2 \text{Var}\,[\overline{M}'.(w)] + \left(\frac{\overline{\Re}.(w)}{\overline{S}'.(w)}\right)^2 \text{Var}\,[\overline{S}'.(w)] \quad \text{(B1)}$$

where

$$\text{Var}\,[\overline{M}'.(w)] = \frac{1}{V}\text{Var}\,[M'_v(w)] \quad \text{(B2)}$$

(similar for S). Note that Var $[\Re_u(w)]$ does not exist because $\Re_u(w)$ does not exist; the measurements of $S_u(w)$ and $M_v(w)$ were not paired.

For analysis of variance (ANOVA) to test the significance of the effect of waveform k on $\Re$, the mean-square of the treatment (waveform) MSTr is calculated in the usual way (we replace the waveform vector w with the scalar index k):

$$\text{MSTr} = \frac{U}{K-1}\sum_{k=1}^{K}[\overline{\Re}.(k) - \overline{\Re}.(\cdot)]^2 \quad \text{(B3)}$$

where $K = 10$ is the number of waveforms. However, because $\Re_u(k)$ does not exist, the mean-square error MSE cannot be calculated in the usual way:

$$\text{MSE} = \frac{1}{K(U-1)}\sum_{k=1}^{K}\sum_{u=1}^{U}[\Re_u(k) - \overline{\Re}.(k)]^2.$$

Nevertheless, if we note that MSE is the mean of the variance of all K waveforms

$$\text{MSE} = \frac{1}{K}\sum_{k=1}^{K}\text{Var}\,[\Re_u(k)]$$

and that Var $[\overline{\Re}.(k)]$ = Var $[\Re_u(k)]/U$ if $\Re_u(k)$ did exist (assuming the independence of the replicates r), we can calculate the error as

$$\text{MSE} = \frac{U}{K}\sum_{k=1}^{K}\text{Var}\,[\overline{\Re}.(k)]$$

where Var $[\overline{\Re}.(k)]$ is given by (B1). The ANOVA test then proceeds with f = MSTr/MSE with $K - 1 = 9$ degrees of freedom (dof) in the numerator and $K(U-1) = 20$ dof in the denominator.

Fig. 18 shows that the magnitude estimates $\Gamma_r(w)$ contain two sources of experimental error: (1) error in determining $M_v(w)$ and (2) error in estimating Γ when $\overline{M}'.(w)$ is re-presented to O. (In the following discussion we will drop the prime notation for clarity so that $\overline{M}.(w)$ means $\overline{M}'.(w)$, the mean of the three drift-corrected replications v of maximal current without discomfort $M_v(w)$ for waveform w). These two error sources are independent; each is the result of measurement replication in different random orders. The total variance in $\Gamma_r(w)$ is therefore the sum of the component variances, with appropriate

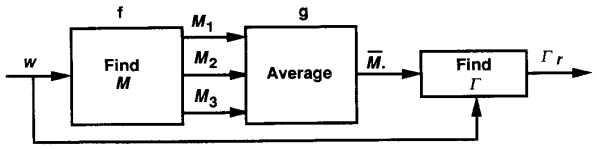

Fig. 18. The estimated dynamic range Γ contains two sources of experimental error: 1) nonpeatability in finding the maximal current without discomfort M and (2) nonrepeatability in finding the maximal magnitude Γ at current M. Γ depends on both the current M and the waveform w.

scaling. We model the **MAG** experiments as follows:

$$M_v(w) = f(w) + \alpha_v$$
$$\Gamma_r = g[w, \overline{M}.(w)] + \beta_r \quad \text{(B4)}$$

where

$$\overline{M}.(w) = \frac{1}{V}\sum_{v=1}^{V} M_v(w)$$

and α and β are normal random variables with mean 0 and variance σ_f^2 and σ_g^2, respectively, f and g are the "true" functions for M and Γ in the absence of experimental error, and $v(1 \ldots V = 3)$ and $r(1 \ldots R = 5)$ are the replicates of the M and Γ experimental trials. Because α and β are independent,

$$\text{Var}\,(\Gamma_r) = \text{Var}\,[g(w), \overline{M}.)] + \text{Var}\,(\beta_r)$$

where $\overline{M}.$ is assumed to mean $\overline{M}.(w)$ for clarity. Because the relationship between Γ and M is approximately linear in the region of interest near $\psi(w_{\text{REF}}) = 20$,

$$\text{Var}\,(\Gamma_r) = \left(\frac{\partial\psi}{\partial w}\right)^2 \text{Var}\,(w) + \left(\frac{\partial\psi}{\partial\overline{M}.}\right)^2 \text{Var}\,(\overline{M}.) + \sigma_g^2$$

but because w is constant and because of (B4),

$$\text{Var}\,(\Gamma_r) = \frac{1}{V}\left(\frac{\partial\psi}{\partial\overline{M}.}\right)^2 \sigma_f^2 + \sigma_g^2$$

where the model variances are experimentally approximated by

$$\sigma_f^2 \approx \frac{1}{V-1}\sum_{v=1}^{V}[M_v(w) - \overline{M}.(w)]^2$$
$$\sigma_g^2 \approx \frac{1}{R-1}\sum_{r=1}^{R}[\Gamma_r(w) - \overline{\Gamma}.(w)]^2$$

and the derivative is experimentally approximated by

$$\frac{\partial\psi}{\partial\overline{M}.} \approx \frac{\psi(M) - \psi(I_{\text{LOW}})}{M - I_{\text{LOW}}}$$

where the LOW current $I_{\text{LOW}} = S + 0.75(M - S)$ with the REF waveform.

For the mean $\overline{\Gamma}.(w)$ of all $R = 5$ replications, the variance due to β is reduced by a factor of R, but the error due to α is not reduced further because all R replicates of

Γ use the same value of $\overline{M}.(w)$. Therefore,

$$\text{Var}\,(\overline{\Gamma}.) = \frac{1}{V}\left(\frac{\partial\psi}{\partial\overline{M}.}\right)^2 \sigma_f^2 + \frac{1}{R}\sigma_g^2 \tag{B5}$$

and the standard errors in Table I are the square root of this quantity.

To use ANOVA for testing the significance of Γ effects, MSTr is calculated similarly to (B3). However, MSE must be carefully constructed for a valid f test. Based on the model in (B4), it can be shown that the expected value of MSTr is

$$E[\text{MSTr}] = \frac{R}{K-1}\sum_{k=1}^{K}\left(g(k) - \frac{1}{K}\sum_{k=1}^{K} g(k)\right)^2 + \frac{R}{V}\left(\frac{\partial\psi}{\partial\overline{M}.}\right)^2 \sigma_f^2 + \sigma_g^2.$$

If the null hypothesis H_0 is true (there is no effect of waveform k on Γ, i.e., $\Gamma(k_1) = \Gamma(k_2) = \cdots = \Gamma(k_K)$), then the first term (the real effect) is zero. Therefore, we construct MSE so that $f = \text{MSTr}/\text{MSE} = 1$ when H_0 is true:

$$\text{MSE} = \frac{R}{V}\left(\frac{\partial\psi}{\partial\overline{M}.}\right)^2 \sigma_f^2 + \sigma_g^2$$

There are $K - 1 = 9$ dof for MSTr and between $K(V - 1) = 20$ and $K(R - 1) = 40$ dof for MSE. We use 20 dof for a conservative test.

For the **Gradient** experiment, the model for the full factorial analysis is

$$\begin{aligned}\overline{\Gamma}.(w) = {} & a_0 \\ & + (a_1x_1 + a_2x_2 + a_3x_3 + a_4x_4)/2 \\ & + (a_{12}x_1x_2 + a_{13}x_1x_3 + a_{14}x_1x_4 + a_{23}x_2x_3 \\ & + a_{24}x_2x_4 + a_{34}x_3x_4)/2 \\ & + (a_{123}x_1x_2x_3 + a_{124}x_1x_2x_4 + a_{134}x_1x_3x_4 \\ & + a_{234}x_2x_3x_4)/2 \\ & + (a_{1234}x_1x_2x_3x_4)/2\end{aligned}$$

where $x_1 - x_4$ are linearly scaled versions of NPB, PRR, W, and IPI and take on values of only -1 and 1 [34]. The standard errors of the effects a are

$$\text{SE}(a) = \left\{\frac{1}{4K}\sum_{k=1}^{K}\text{Var}\,[\overline{\Gamma}.(k)]\right\}^{1/2}$$

where $K = 2^4 = 16$ waveforms and $\text{Var}\,[\overline{\Gamma}.(k)]$ is given by (B5).

In the single-variable effect experiments **MagNPB, MagPRR, MagW,** and **MagIPI,** the mean $\overline{\Re}\,.,.\,(k)$ value is averaged *geometrically* over the O observers o

$$\overline{\Re}\,.,.\,(k) = \left[\prod_{o=1}^{O}\Re_{.,.,o}(k)\right]^{1/O} \tag{B6}$$

because while their trends are similar, their absolute levels are quite different; the means $\overline{\Re}_{.,.,o}(\cdot)$ over all values of PRR vary over a 3:1 range. The error bars in Figs. 13–16 show the SE of the mean over all 6 or 7 O's, 10 waveforms k, and replications:

$$\text{SE}[\overline{\Gamma}_{.,.}(\cdot)] = \left\{\frac{\frac{1}{K}\sum_{k=1}^{K}\left(\frac{1}{O}\sum_{o=1}^{O}\text{Var}\,[\overline{\Gamma}_{.,.,o}(k)] + \frac{1}{O-1}\sum_{o=1}^{O}[\overline{\Gamma}_{.,.}(k) - \overline{\Gamma}_{.,.,o}(k)]^2\right)}{O}\right\} \tag{B7}$$

where the Var term is given by (B5); a similar expression combined with (B1) calculates $\text{SE}[\overline{\Re}_{.,.}(\cdot)]$. The addition of variances in the numerator is justified by the assumption that the errors due to O's and errors due to replications are independent.

Acknowledgment

We thank Dr. J. Dannemiller (Dept. of Psychology), Dr. M. Clayton (Dept. of Statistics), and Dr. K. Neuwirth (Academic Computing Center) for their assistance with psychophysical and statistical methods.

References

[1] K. A. Kaczmarek, J. G. Webster, P. Bach-y-Rita and W. J. Tompkins, "Electrotactile and vibrotactile displays for sensory substitution systems," *IEEE Trans. Biomed. Eng.*, vol. 38, pp. 1-16, 1991.

[2] A. Y. J. Szeto and F. A. Saunders, "Electrocutaneous stimulation for sensory communication in rehabilitation engineering," *IEEE Trans. Biomed. Eng.*, vol. BME-29, pp. 300-308, 1982.

[3] A. Y. J. Szeto and R. R. Riso, "Sensory feedback using electrical stimulation of the tactile sense," in *Rehabilitation Engineering*, R. V. Smith and J. H. Leslie Jr., Eds. Boca Raton, FL: CRC Press, 1990, pp. 29-78.

[4] P. Bach-y-Rita, *Brain Mechanisms in Sensory Substitution.* New York: Academic, 1972.

[5] C. C. Collins, "On mobility aids for the blind," in *Electronic Spatial Sensing for the Blind*, D. H. Warren and E. R. Strelow, Eds. Dordrecht, The Netherlands: Matinus Nijhoff, 1985, pp. 35-64.

[6] C. M. Reed, N. I. Durlach, and L. D. Bradia, "Research on tactile communication of speech: A review," *AHSA Monographs*, vol. 20, pp. 1-23, 1982.

[7] C. E. Sherrick, "Basic and applied research on tactile aids for deaf people: Progress and prospects," *J. Acoust. Soc. Amer.*, vol. 75, pp. 1325-1342, 1984.

[8] A. Y. J. Szeto and K. M. Christensen, "Technological devices for deaf-blind children: Needs and potential impact," *IEEE Eng. Med. Biol. Mag.*, vol. 7, no. 3, pp. 25-29, 1988.

[9] C. C. Collins and J. M. J. Madey, "Tactile sensory replacement," in *Proc. San Diego Biomed. Symp.*, vol. 13, 1974, pp. 15-26.

[10] C. A. Phillips, "Sensory feedback control of upper- and lower-extremity motor prostheses," *CRC Crit. Rev. Biomed. Eng.*, vol. 16, pp. 105-140, 1988.

[11] R. R. Riso, "Sensory augmentation for enhanced control of FNS systems," in *Ergonomics in Rehabilitation*, A. Mital, Ed. New York: Taylor and Francis, 1988, pp. 253-271.

[12] F. A. Saunders, "Information transmission across the skin: High-resolution tactile sensory aids for the deaf and the blind," *Int. J. Neurosci.*, vol. 19, pp. 21-28, 1983.

[13] F. A. Saunders, "Electrocutaneous displays," in *Proc. Conf. Cutan. Comm. Sys. Dev.*, F. A. Geldard, Ed. Psychonomic Soc., 1973, pp. 20-26.

[14] S. S. Stevens, "The psychophysics of sensory functions," in *Sensory*

Communication. W. Rosenblith, Ed. Cambridge: M.I.T. Press, 1962, pp. 1-33.
[15] G. B. Rollman, "Electrocutaneous stimulation," in *Proc. Conf. Cutan. Comm. Syst. Dev.*, F. A. Geldard, Ed. Psychonomic Soc., 1973, pp. 38-51.
[16] D. V. Cross, B. Tursky, and M. Lodge, "The role of regression and range effects in determination of the power function for electric shock," *Percept. Pschophys.*, vol. 18, pp. 9-14, 1975.
[17] R. M. Sachs, J. D. Miller, and K. W. Grant, "Perceived magnitude of multiple electrocutaneous pulses," *Percept. Psychophys.*, vol. 28, pp. 255-262, 1980.
[18] P. McCallum and H. Goldberg, "Magnitude scales for electrocutaneous stimulation," *Percept. Psychophys.*, vol. 17, pp. 75-78, 1975.
[19] K. A. Kaczmarek, K. M. Kramer, J. G. Webster, and R. G. Radwin, "A 16-channel 8-parameter waveform electrotactile stimulation system," *IEEE Trans. Biomed. Eng.*, vol. 38, pp. 933-943, 1991.
[20] M. P. Lynch, R. E. Eilers, D. K. Oller, and L. Lavoie, "Speech perception by cogenitally deaf subjects using an electrocutaneous vocoder," *J. Rehab. Res. Dev.*, vol. 25, pp. 41-50, 1988.
[21] F. A. Saunders, *Tacticon 1600 Electrotactile Sensory Aid for the Deaf: User's Guide.* Concord, CA: Tacticon Corp., 1986.
[22] K. A. Kaczmarek, "Optimal Electrotactile Stimulation Waveforms for Human Information Display," Ph.D. thesis, Dept. Elec. Comput. Engineering, Univ. of Wisconsin-Madison, 1991.
[23] L. E. Marks, "Psychophysical measurement: procedures, tasks, scales," in *Social Attitudes and Psychophysical Measurement*, B. Wegener, Ed. Hillsdale, NJ: Lawrence Erlbaum Assoc., 1982, pp. 43-71.
[24] R. H. Gibson, "Electrical stimulation of pain and touch," in *The Skin Senses*, D. R. Kenshalo, Ed. Springfield, IL: Charles C Thomas, 1968, pp. 233-260.
[25] P. H. Gorman and J. T. Mortimer, "The effect of stimulus parameters on the recruitment characteristics of direct nerve stimulation," *IEEE Trans. Biomed. Eng.*, vol. BME-30, pp. 407-414, 1983.
[26] C. C. Collins, "Tactile television—mechanical and electrical image projection," *IEEE Trans. Man-Mach. Sys.*, vol. MMS-11, pp. 65-71, 1970.
[27] M. Lodge, "Magnitude scaling: Quantitative measurement of opinions," in *Sage University Paper series on Quantitative Applications in the Social Sciences*, J. L. Sullivan and R. G. Niemi, Eds. Beverly Hills, CA: Sage Publications, 1984, pp. 1-87.
[28] D. V. Cross, "On judgements of magnitude," in *Social Attitudes and Psychophysical Measurement*, B. Wegener, Ed. Hillsdale, NJ: Lawrence Erlbaum Assoc., 1982, pp. 73-88.
[29] R. T. Verrillo, "Psychophysics of vibrotactile stimulation," *J. Acoust. Soc. Amer.*, vol. 77, pp. 225-232, 1985.
[30] A. Y. J. Szeto, "Relationship between pulse rate and pulse width for a constant-intensity level of electrocutaneous stimulation," *Ann. Biomed. Eng.*, vol. 13, pp. 373-383, 1985.
[31] C. C. Collins and F. A. Saunders, "Pictorial display by direct electrical stimulation of the skin," *J. Biomed. Syst.*, vol. 1, pp. 3-16, 1970.
[32] F. A. Saunders, "Recommended procedures for electrocutaneous displays," in *Functional Electrical Stimulation: Applications in Neural Prostheses*, F. T. Hambrecht and J. B. Reswick, Eds. New York: Marcel Dekker, 1977, pp. 303-309.
[33] M. Solomonow and D. Prados, "Further evidence on learning in the tactile sense," in *Proc. IEEE Frontiers Eng. Health Care*, 1982, pp. 339-342.
[34] G. E. P. Box, W. G. Hunter and J. S. Hunter, *Statistics for Experiments.* New York: Wiley, 1978.
[35] W. Volk, *Applied Statistics for Engineers.* New York: McGraw-Hill, 1958.

Kurt A. Kaczmarek (S'82-M'82-S'83-M'83-S'86-M'92) received the B.S. degree from the University of Illinois-Urbana, in 1982 and the M.S. and Ph.D. degrees from the University of Wisconsin-Madison, in 1984 and 1991, respectively, all in electrical engineering. For his M.S. thesis he developed a vision-replacement system that sequentially presents image segments from a digital camera to a blind user via a vibrotactile display *IEEE Trans. Biomed. Eng.*, vol. BME-32, pp. 602-608, 1985.

From 1984 to 1986 he developed advanced medical product sterilization techniques at Baxter International, Round Lake, IL. The present paper represents the largest experimental section of his Ph.D. thesis, which also includes sections on electrotactile sensory adaptation and on the voltage-current characteristics of the electrotactile electrode-skin interface. This research supported the development of a tactile feedback system for the insensate hand. He is a contributing author to *Interfacing Sensors to the IBM PC* (W. J. Tompkins and J. G. Webster, Eds., Englewood Cliffs, NJ: Prentice-Hall, 1988). His interest areas include sensory substitution, medical instrumentation, somatosensory physiology, psychophysics, and physiological modeling.

John G. Webster (M'59-SM'69-F'86) received the B.E.E. degree from Cornell University, Ithaca, NY, in 1953, and the M.S.E.E. and Ph.D. degrees from the University of Rochester, Rochester, NY, in 1965 and 1967, respectively.

He is Professor of Electrical and Computer Engineering at the University of Wisconsin-Madison. In the field of medical instrumentation he teaches undergraduate, graduate, and short courses, and does research on electrical impedance tomography, tactile sensors, electrodes, and biopotential amplifiers. He is author of *Transducers and Sensors*, An IEEE/EAB Individual Learning Program (Piscataway, NJ: IEEE, 1989). He is coauthor, with B. Jacobson, of *Medicine and Clinical Engineering* (Englewood Cliffs, NJ: Prentice-Hall, 1977), and with R. Pallás-Areny, of *Sensors and Signal Conditioning* (New York: Wiley, 1991). He is editor of *Encyclopedia of Medical Devices and Instrumentation* (New York: Wiley, 1988), *Tactile Sensors for Robotics and Medicine* (New York: Wiley, 1988), *Electrical Impedance Tomography* (Bristol, England: Adam Hilger, 1990), *Teaching Design in Electrical Engineering* (Piscataway, NJ: Educational Activities Board, IEEE, 1990), *Prevention of Pressure Sores: Engineering and Clinical Aspects* (Bristol, England: Adam Hilger, 1991), and *Medical Instrumentation: Application and Design, Second Edition* (Boston: Houghton Mifflin, 1992). He is coeditor, with A. M. Cook, of *Clinical Engineering: Principles and Practices* (Englewood Cliffs, NJ: Prentice-Hall, 1979) and *Therapeutic Medical Devices: Application and Design* (Englewood Cliffs, NJ: Prentice-Hall, 1982), with W. J. Tompkins, of *Design of Microcomputer-Based Medical Instrumentation* (Englewood Cliffs, NJ: Prentice-Hall, 1981) and *Interfacing Sensors to the IBM PC* (Englewood Cliffs, NJ: Prentice-Hall, 1988), and A. M. Cook, W. J. Tompkins, and G. C. Vanderheiden, of *Electronic Devices for Rehabilitation* (London: Chapman & Hall, 1985).

Dr. Webster has been a member of the IEEE-EMBS Administrative Committee and the NIH Surgery and Bioengineering Study Section. He has been Associate Editor, Medical Instrumentation, of the IEEE Transactions on Biomedical Engineering, and Chairman of the IEEE-EMBS Fellow Committee.

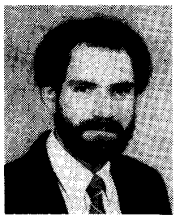

Robert G. Radwin (S'84-M'85) received the B.S.E. degree in electrical engineering from the Polytechnic Institute of New York, Brooklyn, in 1975, and the M.S. degrees in electrical and computer engineering and in bioengineering, from The University of Michigan, Ann Arbor, MI, in 1979, and the Ph.D. degree in industrial and operations engineering at The University of Michigan, Ann Arbor, MI, in 1986. He was appointed as a Postdoctoral Research Fellow at the Center for Ergonomics, Ann Arbor, MI, in 1987.

He is currently an Associate Professor at the University of Wisconsin-Madison in the Department of Industrial Engineering where he conducts research and teaches in the areas of ergonomics, human factors engineering, and biomedical engineering. He is actively studying the causes and prevention of cumulative trauma disorders in manual work. He is developing electronic instruments and analytical methods for assessing exposure to physical stress in the workplace including repetitive motion, forceful exertions, contact stress, postural stress, exposure to cold temperature, and vibration. He is also investigating manual performance deficits associated with peripheral neuropathy.

Dr. Radwin received a Presidential Young Investigator Award from the National Science Foundation and a Special Emphasis Center Award from the National Institute for Occupational Safety and Health. He is a member of Alpha Pi Mu, Eta Kappa Nu, and Sigma Xi.